E. Nikoumanesh [ORCID] ; R. Poling-Skutvik [✉] [ORCID]

Check for updates

CrossMark

View Online

Export Citation

28 July 2023 15:49:50

The effect of thixotropy on the yield transition in reversible, colloidal gels

View Online   Export Citation   CrossMark

E. Nikoumanesh [iD] and R. Poling-Skutvik[a) [iD]

AFFILIATIONS

Department of Chemical Engineering, University of Rhode Island, Kingston, Rhode Island 02881, USA

Note: This paper is part of the 2023 JCP Emerging Investigators Special Collection.
[a)] Author to whom correspondence should be addressed: ryanps@uri.edu

ABSTRACT

Thixotropic yield-stress fluids (TYSFs) are a unique class of materials whose properties are affected by both shear rate and shear history. When sheared, these materials undergo a transition from an elastic solid to a viscoelastic fluid, which is accompanied by a structural transition that slowly recovers upon the cessation of shear. The strong interdependence between structure, dynamics, and rheological properties in TYSFs make it challenging to identify the fundamental physics controlling these phenomena. In this study, we vary the ionic strength of a suspension of cellulose nanocrystals (CNC) to generate model TYSFs with tunable moduli and thixotropic kinetics. We use a novel rheological protocol—serial creep divergence—to identify the physics underlying the yield transition and recovery of CNC gels. Our protocol identifies a critical transition that bifurcates the solid-like and fluid-like regimes of the gels to precisely determine the yield stress of these materials even in the presence of thixotropic effects. Additionally, the thixotropic kinetics collapse onto a single master curve, which we fit to a transient solution to a coupled diffusion–aggregation model. Our work thereby identifies the underlying physicochemical mechanisms driving yielding and thixotropic recovery in attractive colloidal gels.

28 July 2023 15:49:50

I. INTRODUCTION

Yield-stress fluids are found in a wide variety of materials from cosmetics and paints to construction materials and drug delivery systems.[1–3] When these complex fluids are exposed to low stresses, they act like a solid to resist deformation, but at higher stresses, they flow like a liquid to viscously dissipate energy. This transition from elastic deformation to viscous flow can be defined as a yield transition characterized by a specific yield stress. How to define this yield stress, however, continues to be debated. Identifying the yield stress through a physically precise method is essential to design materials with desired mechanical properties and to predict their flow behavior under processing conditions.[4,5]

Over a century ago,[6] Bingham and colleagues introduced the concept of a yield-stress fluid, proposing that once the yield stress σ_y is exceeded under steady shear, the material will flow as a Newtonian fluid with a constant viscosity. Herschel and Bulkley[7] extended this concept by modifying the relationship between shear stress σ and shear rate $\dot{\gamma}$ to incorporate a non-Newtonian viscosity according to $\sigma = \sigma_y + K\dot{\gamma}^n$, where K and n are adjustable model parameters that

define the effective viscosity of the fluid. Refinements to our understanding of yield-stress fluids extended the yield transition from simple steady shear measurements to oscillatory deformations[8–10] and transient start-up shear,[11,12] in which the yield stress is determined by the crossover between the storage and loss moduli or through an overshoot in the transient stress response, respectively. Microstructural changes and spatial heterogeneities underlying the yield transition can be investigated through various experimental techniques, such as confocal microscopy, nuclear magnetic resonance spectroscopy, and ultrasound.[13–15] Even with these significant experimental and theoretical advances, there remains significant ambiguity over how to precisely define and measure σ_y. For instance, depending on the measurement geometry, the experimental protocol, and shear history, σ_y can vary over an order of magnitude.[10,16–19] Furthermore, for many yield-stress fluids, the yield transition occurs concomitant with a second phenomenon—thixotropy. Thixotropy is characterized by a time-dependent recovery of fluid structure and increased viscoelasticity after being subjected to shear stress.[20–22] The dependence on shear history introduced by thixotropy results in additional ambiguity over "the" yield transition for thixotropic yield-stress fluids (TYSFs).

One canonical class of TYSF—gels—possess a percolated structure controlled by the interparticle interactions and dynamics of a dispersed phase suspended in a continuous fluid matrix. Gels can be formed by a wide range of components, including small molecules,[23] colloidal particles,[24] biomacromolecules,[25] polymers,[26] and complex mixtures of the above.[27] Colloidal gels, in particular, have attracted significant interest owing their to importance in a diverse range of applications. In attractive colloidal systems, the sol–gel transition occurs once the colloidal particles self-assemble into a fractal cluster that percolates the sample.[28] A comparable rigidity percolation[29] transition can occur at increasing volume fractions to generate a mechanically robust gel even from softer particles with flexible bonds. As a result of these percolating clusters, colloidal gels become highly elastic with a modulus that scales with particle volume fraction and the strength of attractive interactions.[30] The increase in elastic modulus leads to an increase in σ_y so that stiffer gels require larger stresses to flow.[31] Indeed, for many applications, gels must be processed under flow, during which the applied shear begins to remodel or destroy the percolating structure.[32] As a result, colloidal gels often experience significant changes to their mechanical properties during the yield transition, only sufficiently recovering their elasticity over periods of quiescent rest. How gels recover their mechanical properties is essential to their performance in scientific and industrial applications, but the physical mechanisms relating local structural transitions[33–35] to yielding and thixotropy remain ambiguous and system specific.

In this study, we investigate yielding in the presence of thixotropy to unambiguously define the yield stress σ_y and to gain insight into the physical mechanisms controlling these related phenomena. We use suspensions of cellulose nanocrystals (CNCs) as model TYSFs,[36–38] in which the yield stress is controlled by the addition of salt. The CNCs are negatively charged rod-like colloidal particles that form stable aqueous suspensions. The presence of salt in the suspension causes the charged surface of CNCs to become screened, reducing their repulsive interactions to induce gelation.[39–41] Our study employs a novel rheological protocol, which we term serial creep divergence (SCD), to investigate the correlation between the CNC dynamics and the yielding and recovery behavior of the network. This new protocol allows us to precisely track the evolution of the gel structure over time and provides insights into the mechanisms that govern its yielding behavior. We identify a critical transition that bifurcates the solid-like and fluid-like regimes, allowing us to precisely and unambiguously determine σ_y even in the presence of thixotropic effects. In addition, our novel SCD protocol extracts the kinetics of structural recovery, which we explain through a coupled diffusion–aggregation model. With these findings, we demonstrate the potential of SCD to identify physicochemical mechanisms underlying the rheological properties of colloidal gels and other classes of complex fluids.

II. MATERIALS AND METHODS

A. Materials

Cellulose nanocrystals were purchased from CelluForce (Montreal, Canada) as a dry powder. According to the manufacturer, the CNCs have a nominal size between 120 and 200 nm. Using dynamic light scattering (DLS), we found that the CNCs have a diffusivity of $D_0 = 2.5 \pm 0.2~\mu m^2/s$ corresponding to a hydrodynamic diameter

of 195 ± 22 nm and confirming that the CNCs are well dispersed in solution. Additionally, the ζ-potential of the CNC was found to be -39 ± 1 mV, in good agreement with literature values.[42–44] Potassium chloride was purchased from Fisher Scientific.

B. Gel preparation

Dry CNCs were dispersed in deionized (DI) water at a concentration of 5 wt. % and homogenized on a stir plate for 4 hours. The resulting suspension was optically clear, indicating a homogeneous suspension of the CNC. A salt stock solution was prepared by dissolving KCl in DI at a concentration of 5M. Finally, the CNC stock was diluted with DI water and combined with the salt stock solution to achieve KCl concentrations ranging from 1 to 100 mM and a CNC concentration of 3 wt. %. The gels were allowed to homogenize overnight on a tube roller. A schematic of the preparation procedure is shown in Fig. 1.

C. Rheology

Rheological measurements were conducted using a TA Instruments HR20 rheometer, equipped with 60 mm diameter cone-and-plate and parallel plate geometries. Due to the stiffness of most gels, we were unable to compress them to the required height for the cone geometry in our experiments. Therefore, we utilized parallel plate geometry for the majority of our experiments with a sample thickness of 1 mm. The use of a solvent trap was employed to reduce evaporation during the experiments. To further mitigate evaporation, the edges of the samples were coated with mineral oil. All measurements were conducted at a constant temperature of $T = 25~^\circ C$.

Oscillatory experiments were performed to identify the frequency response and yielding characteristics of these materials. To reduce loading effects, the gels were initially oscillated after loading and trimming at 100% strain for 1 min at a frequency $\omega = 10~s^{-1}$. Then, a series of amplitude sweeps were applied to the sample, starting from a low strain to a high strain, followed by the reverse, going from a high to a low strain amplitude. For the frequency sweeps, we select a strain well within the linear viscoelastic (LVE) region and measure the moduli as a function of frequency in both increasing and decreasing directions. To gain further insight into yielding behavior, we conduct serial creep divergence (SCD) measurements.[45] In SCD, samples are loaded onto the rheometer and initially yielded by applying a constant shear rate $\dot{\gamma} = 100~s^{-1}$ for 1 min. This protocol disrupts the underlying structural network in the material and erases previous mechanical history. After this preshearing protocol, the sample is allowed to rest at quiescent conditions for a waiting time t_w after which a stress σ is imposed and the sample compliance is measured. We repeat this procedure, including the preshear, for increasing t_w and σ. Each compliance curve is measured over 1000 s or until the strain reaches 10 000%.

III. RESULTS AND DISCUSSION

A. Linear rheology

We first confirm that the CNC gels act as thixotropic yield-stress fluids using strain amplitude sweeps in which the material is subjected to oscillatory deformation at a constant frequency (Fig. 2). At small strain amplitudes (e.g., $\gamma < 0.1\%$), a representative gel at a
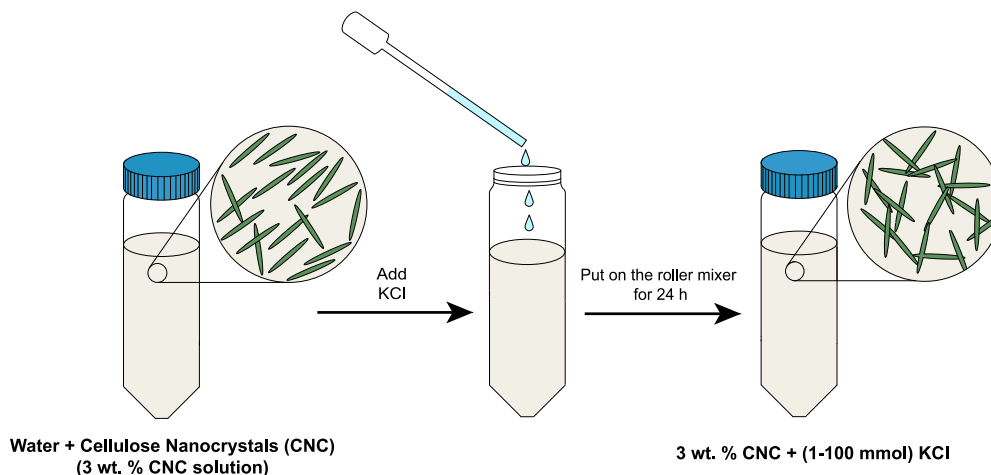
Add
KCl

Put on the roller mixer
for 24 h

Water + Cellulose Nanocrystals (CNC)
(3 wt. % CNC solution)

3 wt. % CNC + (1-100 mmol) KCl

FIG. 1. Schematic of the solution preparation process in which a stock salt solution is combined with an aqueous CNC solution under stirring to achieve 3 wt. % CNC with KCl concentrations ranging from 1 to 100 mM. The addition of salt screens the electrostatic repulsion between CNC particles, causing the particles to aggregate into a percolating network.

salt concentration of 30 mM behaves as a soft solid with the storage modulus G' larger than the loss modulus G''. At higher strains (e.g., $\gamma \gtrsim 10\%$), however, the gel enters a nonlinear regime, and G' drops abruptly. By contrast, G'' initially increases with increasing strain, exhibiting an overshoot at $\gamma \approx 100\%$ before decaying. This decrease in G' and overshoot in G'' are both typical characteristics of yield-stress fluids,[46,47] and gels at all salt concentrations exhibit the same qualitative behavior. After this initial amplitude sweep, we immediately conduct a second amplitude sweep but now in the reverse direction from high to low strains. For non-thixotropic materials, the two amplitude sweeps are expected to agree as the yield transition is reversible.[48–51] For these CNC gels, however, there are significant differences between the moduli measured in the forward and reverse directions. As the strain is reduced, the material returns from its viscous state ($G'' > G'$) to fully recover its elasticity at small
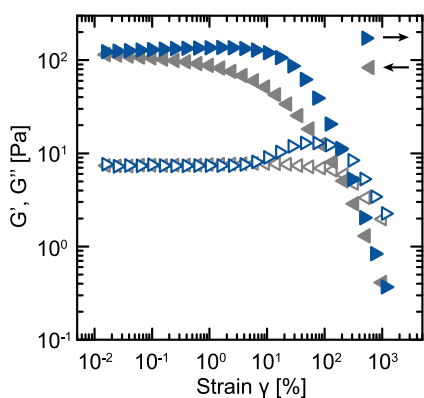
γ, but the recovery follows a dramatically different path. Specifically, there is no overshoot in G'', and G' reaches the linear regime at a significantly lower strain. These differences demonstrate that these CNC gels are thixotropic,[52–55] indicating that the percolating network breaks down under high stress but recovers over time once that stress is removed. As a result, the material properties of the gel strongly depend on the shear history of the sample.

After confirming that these salt-induced CNC gels form thixotropic yield-stress fluids, we investigate how salt affects their linear elasticity. We conduct frequency sweeps within the LVE region (i.e., $\gamma = 0.1\%$) for samples prepared with salt concentrations ranging from 10^0 to 10^3 mM. At low salt concentrations ($c \lesssim 10$ mM), the network behaves like a viscoelastic fluid where the storage and loss moduli increase with frequency but G'' remains larger than G' over the entire frequency range [Fig. 3(a)]. At moderate salt concentrations ($c \approx 10$ mM), we observe an overlap between G' and G'', both of which increase with increasing frequency, following a critical gel-like behavior.[56,57] Finally, at high salt concentrations ($c > 10$ mM), samples behave like a viscoelastic solid where G' is independent of frequency and significantly higher than G''. To identify the gel point in a more rigorous fashion, we plot the loss tangent $\tan(\delta) = G''/G'$ as a function of frequency for the various salt concentrations [Fig. 3(b)]. We observe that $\tan(\delta)$ becomes independent of frequency for $c \approx 10$ mM KCl, which satisfies the Winter–Chambon criterion defining the gel point.[58,59] Finally, we quantify the increase in elasticity with salt concentration by taking G' at $\omega = 10$ rad/s as a representative value and plotting it as a function of c [Fig. 3(c)]. We observe a plateau at low and high salt concentrations, along with a rapid increase near the critical concentration $c = 10$ mM, consistent with the previous literature.[30,60–63] This linear rheology confirms the physical picture that at low salt concentrations, the repulsive forces between CNC particles stabilize the colloidal suspension but are screened at high salt concentrations to aggregate the CNC into a percolating network.[64,65] This percolating network underlies the thixotropic yield stress response that we identified earlier in which the network

FIG. 2. Storage (closed symbols) G' and loss (open symbols) G'' moduli as a function of oscillation strain γ for a 30 mM KCl gel. Data collected with increasing and decreasing γ are shown in blue and gray, respectively. All results were obtained at $\omega = 10$ rad s^{-1}.
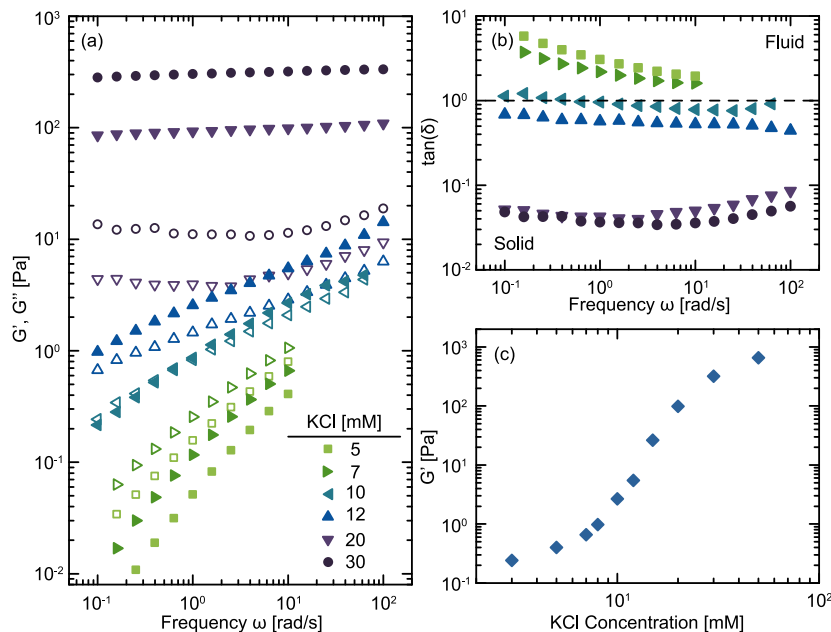
FIG. 3. (a) Storage (closed symbols) G' and loss (open symbols) G'' moduli and (b) $\tan(\delta) = G''/G'$ as a function of frequency ω at various salt concentrations. (c) G' at $\omega = 10$ rad s^{-1} as a function of salt concentration.

breaks under stress to viscously flow and reforms under quiescent conditions.

B. Serial creep divergence (SCD)

Whereas many experimental methods require a choice of $\dot{\gamma}$ to impose a deformation on yield-stress fluids,[16] creep measurements explicitly define the stress imposed on the sample and measure the evolution in strain. We use these measurements to distinguish between fluid-like and solid-like states in a similar method to viscosity bifurcation,[52] except we allow the network to repair under quiescent conditions rather than evolve in steady shear flow. Our methodology, which we call serial creep divergence (SCD), involves pre-shearing the material to break its structure, allowing the gel to quiescently reorganize and rebuild the underlying network over a waiting time t_w and finally applying a stress σ to measure the compliance $J = \gamma/\sigma$ of the material over time (Fig. 4). At short t_w, the CNC gels exhibit a power law increase in compliance, indicating that the sample immediately flows through a combination of viscous dissipation, characterized by the scaling $J \sim t$, and instrument inertia, characterized by the scaling $J \sim t^2$. Although this sample is above the gel point (i.e., $c > 10$ mM), there is insufficient time for the network to recover between yielding events. As t_w increases, the network begins to restructure, and the compliance exhibits an intermediate plateau with delayed yielding. Eventually, after a sufficiently long t_w, the network recovers to fully support the applied stress, resulting in a long-time plateau reflecting solid-like behavior.

The applied stress has a direct impact on the time required for the network to rebuild and support external stresses. For instance,

when $\sigma = 15$ Pa is applied to a $c = 30$ mM sample, the network quickly reorganizes itself to support the stress after ≈ 20 s. At $\sigma = 55$ Pa, however, the network requires a significantly longer time to reorganize, up to 6000 s (Fig. 4). The SCD results demonstrate that as σ increases, the time required for the network to rebuild and support the stress also increases. We attribute this increase in t_w to the fact that the elastic network must reach a higher bond density to support higher stresses.[66] When the applied stress is too high, however, the material cannot form a sufficiently robust network and will always yield regardless of waiting time t_w (see supplementary material). It is important to note that measuring the creep response under such high stress is a challenging task because the material begins to fail at the gel-plate interface (adhesive failure) rather than within the gel (cohesive failure). As a result, the rheometer accelerates rapidly after failure and shuts down for safety. For all measurements shown here, the material fails cohesively so that the creep responses reflect the material properties of the gel. Previous work[67–69] investigated yielding in this high-stress regime and found that increased stress enhances yielding so that colloidal gels yield more rapidly under higher stress. Our work, however, focuses on the yielding behavior of weakened thixotropic gels (i.e., after initial failure) at stresses smaller than their quiescent equilibrium yield stress.

To investigate the relationship between t_w and yielding, we quantify the shift in compliance curves by defining the yield time Δt_y as the difference between the inertial response of the instrument and the time at which $\gamma = 600\%$ (Fig. 4). Although this choice of strain is arbitrary, it effectively separates materials that flow from those that exhibit long-time plateaus in compliance. For all
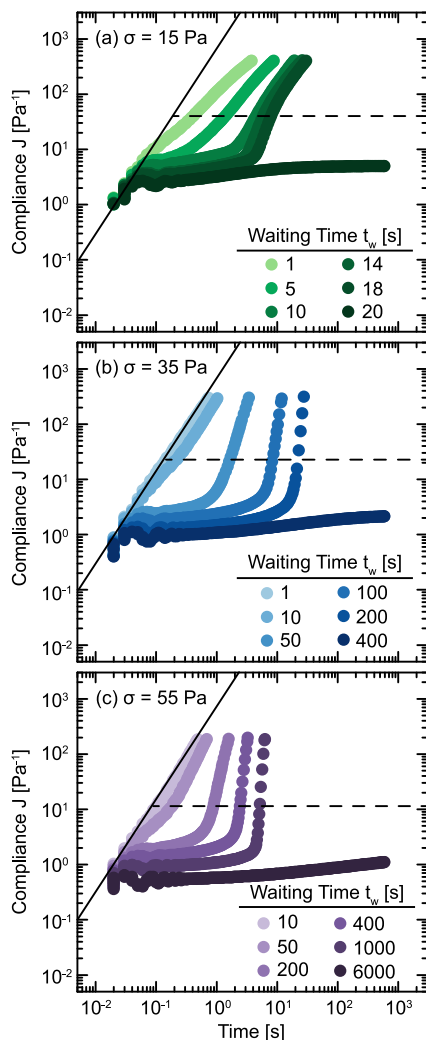
FIG. 4. Compliance $J = \gamma/\sigma$ as a function of time for a $c = 30$ mM sample under applied stresses of (a) 15 Pa, (b) 35 Pa, and (c) 60 Pa at various waiting times t_w. Solid lines indicate an inertial response of the instrument with $J \sim t^2$. Dashed lines indicate the threshold used to quantify the yield time at $\gamma = 600\%$.

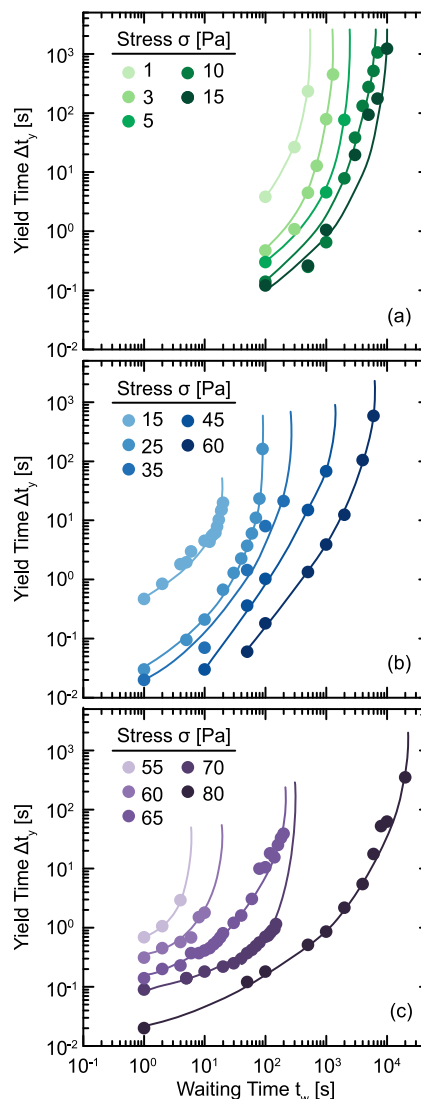**FIG. 5.** Yield time Δt_y as a function of waiting time t_w under different applied stresses for samples with (a) 15 mM, (b) 30 mM, and (c) 50 mM KCl. Colored curves are guides to the eye.

samples, Δt_y increases with waiting time t_w before diverging to infinity (Fig. 5). The time at which Δt_y diverges depends on both salt concentration and applied stress, increasing with stress as the network takes longer to restructure and decreasing with salt concentration as attractive interactions between the CNC become stronger. For these experiments, Δt_y is less than t_w, indicating that the CNC gels are at a quasi-steady state during each creep experiment, minimizing structural changes in the material under flow. The divergence of Δt_y corresponds to the transition between compliance curves exhibiting viscous flow and those that exhibit elastic deformation, reflecting the bifurcating responses observed in Fig. 4. Physically, the divergence Δt_y at a specific t_w identifies the time at which the material has developed a percolating elastic network dense enough

to support the applied stress without exhibiting bulk flow. Therefore, we determine the gel strength unambiguously from the plot by identifying the waiting time at which the divergence occurs. This relationship, however, still depends on both t_w and σ. To appropriately define yielding of these thixotropic materials, we aim to remove the dependence on t_w and identify a critical stress σ_c that always separates elastic deformation from viscous flow.

To define the critical stress σ_c independent of thixotropy, we investigate the relationship between yield time divergence, applied stress, and salt concentration. Specifically, we define the waiting time at which the yield time diverges $t_{Y,\infty}$ and plot it as a function of σ (Fig. 6). We observe that $t_{Y,\infty}$ increases with σ and decreases with c. At high c, the attractive interactions between particles become
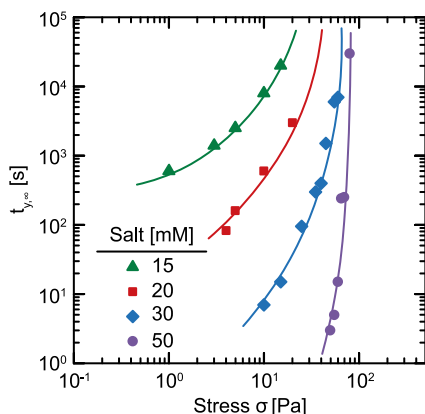
FIG. 6. Long-time yield divergence $t_{y,\infty}$ as a function of stress σ for samples with different salt concentrations. Solid curves are guides to the eye.

stronger, leading to stronger interparticle bonds and faster particle aggregation to generate a dense network in a shorter amount of time. At a critical stress σ_c, $t_{y,\infty}$ diverges as the gel can no longer support stresses beyond this value, even with infinite recovery times. This unique divergence of divergences at σ_c, therefore unambiguously differentiates between stresses that induce flow in the sample and those that can be supported by the underlying strength of the percolated network. We thus propose that σ_c represents a precise definition of the yield stress for these thixotropic fluids.

We compare the critical stress values obtained from SCD to the values determined through other standard methods, such as oscillatory amplitude sweeps and stress growth measurements (Fig. 7). For this comparison, σ_y is defined in oscillatory amplitude sweeps by the crossover between G' and G'' at $\omega = 10$ rad s^{-1} and in stress growth measurements as the maximum stress under steady shear. In SCD, the critical stress σ_c determined by the divergence of $t_{y,\infty}$ defines the yield stress and increases monotonically with salt concentration. The

yield stresses determined from stress growth measurements agree with the SCD values at low salt concentrations but exhibit a non-monotonic dependence that decreases at higher salt concentrations, suggesting that σ_y *decreases* with *increasing* interaction strength and, thus, violating predictions for flocculated suspensions.[1] Finally, the yield stress measured in oscillatory amplitude sweeps increase monotonically like those of SCD but are almost an order of magnitude smaller. These lower values determined under oscillatory deformation may result from activated bond breaking induced by the imposed strain.[70] Thus, we find that SCD defines a yield stress using critical phenomena—divergences and bifurcations—that acts as an effective upper-bound compared to other definitions.

C. Restructuring kinetics

In addition to defining σ_c, these $t_{y,\infty}$ curves exhibit self-similarity across all salt concentrations. To investigate this self-similarity, we collapse the data onto a single curve by normalizing the applied stress by σ_c and $t_{y,\infty}$ by a kinetic time scale τ_0 (Fig. 8). This kinetic time scale was chosen to follow an established scaling law that collapses the growth in the linear rheology with time[71] according to $\tau_0 \sim c^{-8.7}$ where we define $\tau_0 = 1$ s at $c = 30$ mM. With these normalizations, the data collapse onto a single master curve for all salt concentrations, ranging over six decades in time and two decades in stress, confirming that the critical stress σ_c represents a precise definition of the yield stress. The collapse of these data suggests that the physical mechanism underlying the restructure of these gels is independent of salt concentration.

Additionally, the time scale τ_0 required to collapse the data (inset of Fig. 8) relates to the kinetics by which these gels restructure and exhibits a strong decrease as σ_c increases. To investigate these kinetics, we invert the yield divergence to show the growth in the strength of the network as a function of normalized time (Fig. 9). Here, we assume that these gels fail by developing a shear band in which bonds are broken along a plane. Both experimental[72–74] and theoretical[75,76] studies have shown that polymeric and colloidal gels do indeed yield by developing shear bands in which the strain is localized within the sample to an area with a finite width, although
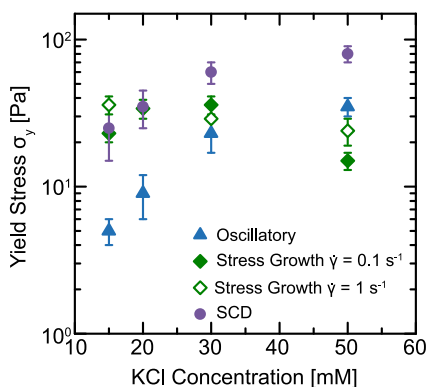

FIG. 7. Yield stress σ_y as a function of salt concentrations extracted from oscillatory amplitude sweeps, transient shear growth measurements at different shear rates $\dot{\gamma}$, and our serial creep divergence protocol.
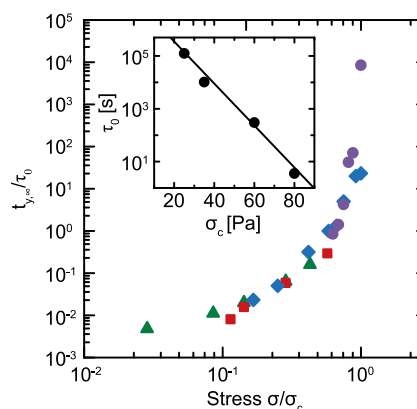

FIG. 8. Master yield curve obtained by normalizing the long-time yield divergence $t_{y,\infty}/\tau_0$ and stress σ/σ_c. *Inset*: normalization time τ_0 as a function of critical stress σ_c. Solid line is the equation $\tau_0 = 10^7 \exp(-\sigma_c/5.5)$.
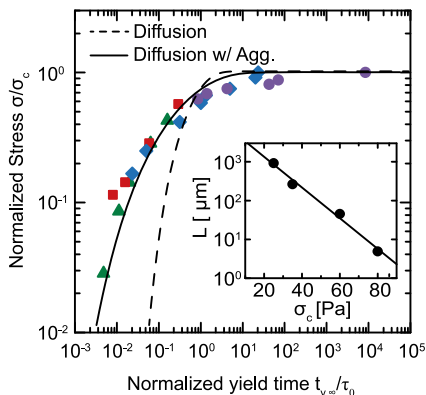
FIG. 9. Normalized stress σ/σ_c as a function of the normalized long-time yield plateau $t_{y,\infty}/\tau_0$ for samples with different salt concentrations. The dashed line is the best fit to a diffusion model [Eq. (2)], and the solid line is the best fit to the diffusion–aggregation model [Eq. (3)]. *Inset*: estimated thickness of the shear band interface L as a function of σ_c. The solid line is equation $L = 8147 \exp(-\sigma_c/11)$.

more complex heterogeneous scenarios have also been observed.[68] For these colloidal gels, such a shear band may be transient[77] or long-lived,[78,79] but under our experimental protocol, we cease shearing immediately after yielding to prevent the rheometer from accelerating and ejecting the sample. Thus, we cannot distinguish between these two scenarios. At a shear band interface, simulations[76] find that there is a decreased particle density and a high shear rate due to the difference in the velocities between the shear bands.[73] Although our rheological measurements do not allow us to directly identify shear bands, our physical assumption is consistent with our observations of cohesive failure, verified by the gel uniformly coating both the top and bottom plate of the rheometer after unloading.

Under this shear band picture, the gel may recovers its properties by repairing the network connectivity across the shear band interface. Colloidal particles would therefore need to transport from the bulk, bind to neighboring particles in the shear band interface, and reform a cohesive percolating network. We initially describe this process by solving Fick's second law in 1D, a partial differential equation relating the spatiotemporal concentration profiles through a diffusivity D, given by

$$\frac{\partial c}{\partial t} = D\frac{\partial^2 c}{\partial x^2}. \qquad (1)$$

We model the shear band interface as a finite slab of thickness $2L$ with boundary conditions $c(x = -L) = c(x = L) = c_s$ and an initial condition $c(t = 0) = 0$, where $x = 0$ is the midplane of the shear band interface and c_s represents the bulk concentration of the equilibrium gel. These boundary conditions assume that the concentration of the dispersed phase, and therefore bond density, is constant within each shear band and fully depleted at the interface. Under quiescent conditions, colloidal particles can transport across the interface to restore the elastic network. We make two assumptions to solve this equation. First, we assume that the local stress σ scales proportionally to c, as expected from the affine network model.[80] Second, we assume that the stress that can be supported by the network is controlled by the concentration at the midplane, which would

be the weakest point of the gel. With these two assumptions, we solve the partial differential equation through standard approaches assuming separation of variables and solving for the boundary and initial conditions. The solution is an infinite sum of eigenmodes, defined by

$$\frac{\sigma_c - \sigma}{\sigma_c} = \frac{4}{\pi}\sum_{n=\text{odd}}^{\infty}\frac{1}{n}\sin\left(\frac{n\pi}{2}\right)\exp\left[-\frac{n^2\pi^2\zeta_0}{4}\left(\frac{t}{\tau_0}\right)\right], \qquad (2)$$

where $\zeta_0 = \tau_0 D/L^2$ is the only fitting parameter. This diffusion argument, however, fails to capture the experimental data (Fig. 9). The colloidal gels exhibit slower kinetics in which the normalized stress increases more gradually with time as compared to the diffusion prediction.

To improve our description of restructuring kinetics, we recognize that the CNC experience strong interparticle attractions that may modify their diffusion into the shear band interface. Previous studies have found that suspensions of attractive colloids aggregate through a diffusion–limited aggregation (DLA) model.[81–83] In this model, colloids form a permanent bond immediately upon contact with another particle, leading to the growth of fractal clusters that follow a universal scaling law $R_g \sim t^\alpha$, where R_g is the radius of gyration of the aggregate and $\alpha = 0.55$ is a universal exponent.[84] According to the Stokes–Einstein relationship, the diffusivity of these fractal clusters scales inversely with R_g. Combining these scaling laws leads to a time-dependent diffusivity $D/D_0 \sim R_g^{-1} \sim t^{-0.55}$, where D_0 is the diffusivity of a single colloidal particle. We incorporate the DLA structural evolution into our diffusion model by setting $D = D_0(t/\tau)^{-0.55}$ in Eq. (1) and proceed to solve the partial-differential equation using the same approach as before, leading to

$$\frac{\sigma_c - \sigma}{\sigma_c} = \frac{4}{\pi}\sum_{n=\text{odd}}^{\infty}\frac{1}{n}\sin\left(\frac{n\pi}{2}\right)\exp\left[-\frac{n^2\pi^2\zeta_0}{4(0.45)}\left(\frac{t}{\tau_0}\right)^{0.45}\right]. \qquad (3)$$

A full derivation of our mathematical solution is presented in the supplementary material. This diffusion–aggregation model excellently fits our experimental findings (Fig. 9) with only a single fitting parameter $\zeta_0 = \tau_0 D_0/L^2$, which relates the normalization time scale τ_0 to the initial particle diffusivity D_0 and thickness L of the shear band interface. Under the assumptions of our model, the excellent agreement between this theoretical prediction and our experimental results suggests that these colloidal gels do indeed yield by developing a shear band within the sample and recover their strength through the diffusion of attractive colloids across the shear band interface. Our rheological measurements, however, do not provide direct structural information on the formation of shear bands, which we aim to determine in future work through particle image velocimetry[33,85] or scattering methods.[86]

As further validation of this model, we convert the arbitrary choice of τ_0 used to collapse the data in Fig. 8 into a physical prediction for the thickness L of the shear band interface using the value $\zeta_0 = 0.37 \pm 0.1$ that best fits our data. Here, we assume that the initial diffusivity is that of a single CNC particle ($D_0 = 2.5\ \mu m^2/s$), as measured by DLS. We note that this choice is likely an overestimate of D_0 as the network may break apart into small clusters under shear instead of completely breaking down into individual particles.[87–89] Using this value for D_0, we find that L decreases from

~1000 μm to 5 μm as the gel strength increases. Even with our simplifying assumptions, these values of L are of the appropriate order of magnitude for our rheological samples, which have a thickness of 1 mm, and are consistent with our observations of cohesive failure. Furthermore, although measuring the thickness of this shear band interface is challenging experimentally, our findings are consistent with predictions derived from a shear transformation zone (STZ) model[75] that show a decrease in the thickness of the shear band interface with increasing interparticle attraction strength. Thus, our diffusion–aggregation model not only captures the kinetics by which the gel strength increases over time but also results in physically meaningful estimates of the thickness of the shear band interface. Future work will aim to investigate the structural transformations occurring within these materials during yielding to precisely identify the presence and size of the shear bands suggested by our findings.

IV. CONCLUSION

We investigate the yield transition in thixotropic colloidal gels using a novel rheological protocol—serial creep divergence (SCD). This protocol elucidates the underlying mechanisms governing the yielding and subsequent recovery of the colloidal gel through a critical bifurcation in the creep response. Our approach leads to an unambiguous definition of the yield stress σ_y according to the divergence of yield times as the material restructures. Additionally, we have shown that these restructuring kinetics are self-similar for all salt concentrations and can be collapsed onto a master curve defined by σ_y and a kinetic timescale τ_0. Furthermore, we show that the growth in the gel strength over time arises from the coupling between colloidal diffusion across the shear band interface and simultaneous aggregation of the attractive colloids. Our experimental results are well-fit by a proposed diffusion–aggregation model, which provides physically reasonable estimates of the thickness of the shear band interface.

With this novel approach and physical insight, our study provides a valuable tool to design and characterize the mechanical behavior of soft materials for use in applications including drug delivery techniques,[90] tissue engineering,[91] and energy storage.[92,93] We expect our SCD protocol to be applicable for a wide variety of complex fluids, enabling researchers to accurately determine the yield transition and critical stress of TYSFs. Specifically, we expect that SCD can help to address the role of particle size, aspect ratio, and geometry on TYSF rheology. Moreover, understanding the impact of various kinds of bonding—electrostatic, covalent, polymer-mediated, etc.—on the mechanical characteristics of gels will significantly improve our ability to design, *a priori*, gels and colloidal suspensions with targeted responses and advanced functionalities.

SUPPLEMENTARY MATERIAL

The supplementary material includes descriptions and results of SCD measurements performed at high stress ($\sigma > \sigma_c$), alternative methods of defining the yield stress σ_y, and a full mathematical derivation of the diffusion–aggregation model.

AUTHOR DECLARATIONS

Conflict of Interest

The authors have no conflicts to disclose.

Author Contributions

E. Nikoumanesh: Formal analysis (lead); Investigation (lead); Methodology (equal); Writing – original draft (equal); Writing – review & editing (equal). **R. Poling-Skutvik**: Conceptualization (lead); Formal analysis (supporting); Funding acquisition (lead); Investigation (supporting); Methodology (lead); Writing – original draft (equal); Writing – review & editing (equal).

DATA AVAILABILITY

The data that support the findings of this study are available from the corresponding author upon reasonable request.

REFERENCES

[1] A. Z. Nelson, K. S. Schweizer, B. M. Rauzan, R. G. Nuzzo, J. Vermant, and R. H. Ewoldt, "Designing and transforming yield-stress fluids," Curr. Opin. Solid State Mater. Sci. **23**, 100758 (2019).

[2] Q. Wang, L. Wang, M. S. Detamore, and C. Berkland, "Biodegradable colloidal gels as moldable tissue engineering scaffolds," Adv. Mater. **20**, 236–239 (2008).

[3] Y. R. Mezzenga and R. Mezzenga, "Design principles of food gels," Nat. Food **1**, 106–118 (2020).

[4] D. Miranda-Nieves and E. L. Chaikof, "Collagen and elastin biomaterials for the fabrication of engineered living tissues," ACS Biomater. Sci. Eng. **3**, 694–711 (2017).

[5] M. E. Del Gado and E. Del Gado, "Mechanics of soft gels: Linear and nonlinear response," in *Handbook of Materials Modeling: Applications: Current and Emerging Materials* (Springer, 2020), pp. 1719–1746.

[6] E. C. Bingham, *Fluidity and Plasticity* (McGraw-Hill, 1922), Vol. 2.

[7] W. H. Herschel and R. Bulkley, "Konsistenzmessungen von Gummi-Benzollösungen," Kolloid-Zeitschrift **39**, 291–300 (1926).

[8] T. Mason, J. Bibette, and D. Weitz, "Yielding and flow of monodisperse emulsions," J. Colloid Interface Sci. **179**, 439–448 (1996).

[9] C. Kugge, N. Vanderhoek, and D. Bousfield, "Oscillatory shear response of moisture barrier coatings containing clay of different shape factor," J. Colloid Interface Sci. **358**, 25–31 (2011).

[10] H. A. Barnes, "The yield stress—A review or '$\pi\alpha\nu\tau\alpha$ $\rho\epsilon\iota$'—everything flows?," J. Non-Newtonian Fluid Mech. **81**, 133–178 (1999).

[11] L. Heymann, S. Peukert, and N. Aksel, "On the solid-liquid transition of concentrated suspensions in transient shear flow," Rheol. Acta **41**, 307–315 (2002).

[12] A. Ragouilliaux, G. Ovarlez, N. Shahidzadeh-Bonn, B. Herzhaft, T. Palermo, and P. Coussot, "Transition from a simple yield-stress fluid to a thixotropic material," Phys. Rev. E **76**, 051408 (2007).

[13] B. Rajaram and A. Mohraz, "Microstructural response of dilute colloidal gels to nonlinear shear deformation," Soft Matter **6**, 2246–2259 (2010).

[14] K. Masschaele, J. Fransaer, and J. Vermant, "Direct visualization of yielding in model two-dimensional colloidal gels subjected to shear flow," J. Rheol. **53**, 1437–1460 (2009).

[15] C. Perge, N. Taberlet, T. Gibaud, and S. Manneville, "Time dependence in large amplitude oscillatory shear: A rheo-ultrasonic study of fatigue dynamics in a colloidal gel," J. Rheol. **58**, 1331–1357 (2014).

[16] M. Dinkgreve, J. Paredes, M. M. Denn, and D. Bonn, "On different ways of measuring "the" yield stress," J. Non-Newtonian Fluid Mech. **238**, 233–241 (2016).

[17] H. A. Barnes and Q. D. Nguyen, "Rotating vane rheometry—A review," J. Non-Newtonian Fluid Mech. **98**, 1–14 (2001).

[18] A. James, D. Williams, and P. Williams, "Direct measurement of static yield properties of cohesive suspensions," Rheol. Acta **26**, 437–446 (1987).

[19] D. Bonn, M. M. Denn, L. Berthier, T. Divoux, and S. Manneville, "Yield stress materials in soft condensed matter," Rev. Mod. Phys. **89**, 035005 (2017).

[20] P. C. Møller, J. Mewis, and D. Bonn, "Yield stress and thixotropy: On the difficulty of measuring yield stresses in practice," Soft Matter **2**, 274–283 (2006).

[21] H. A. Barnes, "Thixotropy—A review," J. Non-Newtonian Fluid Mech. **70**, 1–33 (1997).

[22] R. G. Larson and Y. Wei, "A review of thixotropy and its rheological modeling," J. Rheol. **63**, 477–501 (2019).

[23] L.-C. Yang, Z.-Q. Rong, Y.-N. Wang, Z. Y. Tan, M. Wang, and Y. Zhao, "Construction of nine-membered heterocycles through palladium-catalyzed formal [5+ 4] cycloaddition," Angew. Chem., Int. Ed. **56**, 2927–2931 (2017).

[24] M. Rinaldin, R. W. Verweij, I. Chakraborty, and D. J. Kraft, "Colloid supported lipid bilayers for self-assembly," Soft Matter **15**, 1345–1360 (2019).

[25] B. R. Seo, X. Chen, L. Ling, Y. H. Song, A. A. Shimpi, S. Choi, J. Gonzalez, J. Sapudom, K. Wang, R. C. Andresen Eguiluz *et al.*, "Collagen microarchitecture mechanically controls myofibroblast differentiation," Proc. Natl. Acad. Sci. U. S. A. **117**, 11387–11398 (2020).

[26] I. Bin *et al.*, "Molecular weight dependency of polyrotaxane-cross-linked polymer gel extensibility," Chem. Commun. **52**, 13757–13759 (2016).

[27] M. E. Helgeson, S. E. Moran, H. Z. An, and P. S. Doyle, "Mesoporous organohydrogels from thermogelling photocrosslinkable nanoemulsions," Nat. Mater. **11**, 344–352 (2012).

[28] A. L. R. Bug, S. A. Safran, G. S. Grest, and I. Webman, "Do interactions raise or lower a percolation threshold?," Phys. Rev. Lett. **55**, 1896–1899 (1985).

[29] S. Zhang, L. Zhang, M. Bouzid, D. Z. Rocklin, E. Del Gado, and X. Mao, "Correlated rigidity percolation and colloidal gels," Phys. Rev. Lett. **123**, 058001 (2019).

[30] C. Rueb and C. Zukoski, "Viscoelastic properties of colloidal gels," J. Rheol. **41**, 197–218 (1997).

[31] E. D. Cubuk, R. J. S. Ivancic, S. S. Schoenholz, D. J. Strickland, A. Basu, Z. S. Davidson, J. Fontaine, J. L. Hor, Y.-R. Huang, Y. Jiang, N. C. Keim, K. D. Koshigan, J. A. Lefever, T. Liu, X.-G. Ma, D. J. Magagnosc, E. Morrow, C. P. Ortiz, J. M. Rieser, A. Shavit, T. Still, Y. Xu, N. Nordstrom, P. E. Arratia, R. W. Carpick, D. J. Durian, Z. Fakhraai, D. J. Jerolmack, D. Lee, J. Li, R. Riggleman, K. T. Turner, A. G. Yodh, D. S. Gianola, and A. J. Liu, "Structure-property relationships from universal signatures of plasticity in disordered solids," Science **358**, 1033–1037 (2017).

[32] L. C. Johnson, B. J. Landrum, and R. N. Zia, "Yield of reversible colloidal gels during flow start-up: Release from kinetic arrest," Soft Matter **14**, 5048–5068 (2018).

[33] S. Manneville, "Recent experimental probes of shear banding," Rheol. Acta **47**, 301–318 (2008).

[34] S. Aime, L. Ramos, and L. Cipelletti, "Microscopic dynamics and failure precursors of a gel under mechanical load," Proc. Natl. Acad. Sci. U. S. A. **115**, 3587–3592 (2018).

[35] J. B. Hipp, J. J. Richards, and N. J. Wagner, "Structure-property relationships of sheared carbon black suspensions determined by simultaneous rheological and neutron scattering measurements," J. Rheol. **63**, 423–436 (2019).

[36] A. Rao, T. Divoux, G. H. McKinley, and A. J. Hart, "Shear melting and recovery of crosslinkable cellulose nanocrystal–polymer gels," Soft Matter **15**, 4401–4412 (2019).

[37] M. Fazilati, S. Ingelsten, S. Wojno, T. Nypelö, and R. Kádár, "Thixotropy of cellulose nanocrystal suspensions," J. Rheol. **65**, 1035–1052 (2021).

[38] X. Huang, S. R. Raghavan, P. Terech, and R. G. Weiss, "Distinct kinetic pathways generate organogel networks with contrasting fractality and thixotropic properties," J. Am. Chem. Soc. **128**, 15341–15352 (2006).

[39] X. M. Dong, J.-F. Revol, and D. G. Gray, "Effect of microcrystallite preparation conditions on the formation of colloid crystals of cellulose," Cellulose **5**, 19–32 (1998).

[40] S. Montanari, M. Roumani, L. Heux, and M. R. Vignon, "Topochemistry of carboxylated cellulose nanocrystals resulting from tempo-mediated oxidation," Macromolecules **38**, 1665–1671 (2005).

[41] M.-C. Li, Q. Wu, R. J. Moon, M. A. Hubbe, and M. J. Bortner, "Rheological aspects of cellulose nanomaterials: Governing factors and emerging applications," Adv. Mater. **33**, 2006052 (2021).

[42] P. Keyvani, K. Nyamayaro, P. Mehrkhodavandi, and S. G. Hatzikiriakos, "Cationic and anionic cellulose nanocrystalline (CNC) hydrogels: A rheological study," Phys. Fluids **33**, 043102 (2021).

[43] Y. Boluk and C. Danumah, "Analysis of cellulose nanocrystal rod lengths by dynamic light scattering and electron microscopy," J. Nanopart. Res. **16**, 1–7 (2014).

[44] M. Danesh, A. A. Moud, D. Mauran, S. Hojabr, R. Berry, M. Pawlik, and S. G. Hatzikiriakos, "The yielding of attractive gels of nanocrystal cellulose (CNC)," J. Rheol. **65**, 855–869 (2021).

[45] R. Poling-Skutvik, E. McEvoy, V. Shenoy, and C. O. Osuji, "Yielding and bifurcated aging in nanofibrillar networks," Phys. Rev. Mater. **4**, 102601 (2020).

[46] G. J. Donley, P. K. Singh, A. Shetty, and S. A. Rogers, "Elucidating the G″ overshoot in soft materials with a yield transition via a time-resolved experimental strain decomposition," Proc. Natl. Acad. Sci. U. S. A. **117**, 21945–21952 (2020).

[47] K. Kamani, G. J. Donley, and S. A. Rogers, "Unification of the rheological physics of yield stress fluids," Phys. Rev. Lett. **126**, 218002 (2021).

[48] E. Zaccarelli, "Colloidal gels: Equilibrium and non-equilibrium routes," J. Phys. Condens. Matter **19**, 323101 (2007).

[49] M. J. Solomon and Q. Lu, "Rheology and dynamics of particles in viscoelastic media," Curr. Opin. Colloid Interface Sci. **6**, 430–437 (2001).

[50] J. Mewis and N. J. Wagner, "Thixotropy," Adv. Colloid Interface Sci. **147-148**, 214–227 (2009).

[51] R. Larson, "Constitutive equations for thixotropic fluids," J. Rheol. **59**, 595–611 (2015).

[52] P. Coussot, Q. D. Nguyen, H. Huynh, and D. Bonn, "Viscosity bifurcation in thixotropic, yielding fluids," J. Rheol. **46**, 573–589 (2002).

[53] R. Weltmann, "Thixotropic behavior of oils," Ind. Eng. Chem. Anal. Ed. **15**, 424–429 (1943).

[54] R. Ziegelbaur and J. Caruthers, "Rheological properties of poly (dimethylsiloxane) filled with fumed silica: I. Hysteresis behaviour," J. Non-Newtonian Fluid Mech. **17**, 45–68 (1985).

[55] M. Krystyjan, M. Sikora, G. Adamczyk, A. Dobosz, P. Tomasik, W. Berski, M. Łukasiewicz, and P. Izak, "Thixotropic properties of waxy potato starch depending on the degree of the granules pasting," Carbohydr. Polym. **141**, 126–134 (2016).

[56] K. Te Nijenhuis and H. H. Winter, "Mechanical properties at the gel point of a crystallizing poly (vinyl chloride) solution," Macromolecules **22**, 411–414 (1989).

[57] L. Li and Y. Aoki, "Rheological images of poly (vinyl chloride) gels. 1. The dependence of sol- gel transition on concentration," Macromolecules **30**, 7835–7841 (1997).

[58] F. Chambon and H. Winter, "Stopping of crosslinking reaction in a PDMS polymer at the gel point," Polym. Bull. **13**, 499–503 (1985).

[59] F. Chambon and H. H. Winter, "Linear viscoelasticity at the gel point of a crosslinking PDMS with imbalanced stoichiometry," J. Rheol. **31**, 683–697 (1987).

[60] Y. Xu, A. D. Atrens, and J. R. Stokes, "Liquid, gel and soft glass phase transitions and rheology of nanocrystalline cellulose suspensions as a function of concentration and salinity," Soft Matter **14**, 1953–1963 (2018).

[61] K. A. Whitaker, Z. Varga, L. C. Hsiao, M. J. Solomon, J. W. Swan, and E. M. Furst, "Colloidal gel elasticity arises from the packing of locally glassy clusters," Nat. Commun. **10**, 2237 (2019).

[62] P.-K. Kao, M. J. Solomon, and M. Ganesan, "Microstructure and elasticity of dilute gels of colloidal discoids," Soft Matter **18**, 1350–1363 (2022).

[63] J. Cho, M.-C. Heuzey, A. Bégin, and P. J. Carreau, "Viscoelastic properties of chitosan solutions: Effect of concentration and ionic strength," J. Food Eng. **74**, 500–515 (2006).

[64] H. Fukuzumi, R. Tanaka, T. Saito, and A. Isogai, "Dispersion stability and aggregation behavior of tempo-oxidized cellulose nanofibrils in water as a function of salt addition," Cellulose 21, 1553–1559 (2014).

[65] F. Cherhal, F. Cousin, and I. Capron, "Influence of charge density and ionic strength on the aggregation process of cellulose nanocrystals in aqueous suspension, as revealed by small-angle neutron scattering," Langmuir 31, 5596–5602 (2015).

[66] J. H. Cho and I. Bischofberger, "Yield precursor in primary creep of colloidal gels," Soft Matter 18, 7612–7620 (2022).

[67] J. Sprakel, S. B. Lindström, T. E. Kodger, and D. A. Weitz, "Stress enhancement in the delayed yielding of colloidal gels," Phys. Rev. Lett. 106, 248303 (2011).

[68] T. Gibaud, C. Perge, S. B. Lindström, N. Taberlet, and S. Manneville, "Multiple yielding processes in a colloidal gel under large amplitude oscillatory stress," Soft Matter 12, 1701–1712 (2016).

[69] T. Divoux, M. A. Fardin, S. Manneville, and S. Lerouge, "Shear banding of complex fluids," Ann. Rev. Fluid Mech. 48, 81–103 (2016).

[70] S. Mora, "The kinetic approach to fracture in transient networks," Soft Matter 7, 4908–4917 (2011).

[71] L. Morlet-Decarnin, T. Divoux, and S. Manneville, "Slow dynamics and time composition superposition in gels of cellulose nanocrystals," J. Chem. Phys. 156, 214901 (2022).

[72] P. J. Skrzeszewska, J. Sprakel, F. A. de Wolf, R. Fokkink, M. A. Cohen Stuart, and J. van der Gucht, "Fracture and self-healing in a well-defined self-assembled polymer network," Macromolecules 43, 3542–3548 (2010).

[73] K. A. Erk, J. D. Martin, Y. T. Hu, and K. R. Shull, "Extreme strain localization and sliding friction in physically associating polymer gels," Langmuir 28, 4472–4478 (2012).

[74] T. Bhattacharyya, A. R. Jacob, G. Petekidis, and Y. M. Joshi, "On the nature of flow curve and categorization of thixotropic yield stress materials," J. Rheol. 67, 461–477 (2023).

[75] M. Manning, E. Daub, J. Langer, and J. Carlson, "Rate-dependent shear bands in a shear-transformation-zone model of amorphous solids," Phys. Rev. E 79, 016110 (2009).

[76] J. Colombo and E. Del Gado, "Stress localization, stiffening, and yielding in a model colloidal gel," J. Rheol. 58, 1089–1116 (2014).

[77] T. Divoux, D. Tamarii, C. Barentin, and S. Manneville, "Transient shear banding in a simple yield stress fluid," Phys. Rev. Lett. 104, 208301 (2010).

[78] P. D. Olmsted, "Perspectives on shear banding in complex fluids," Rheol. Acta 47, 283–300 (2008).

[79] J. Paredes, N. Shahidzadeh-Bonn, and D. Bonn, "Shear banding in thixotropic and normal emulsions," J. Phys. Condens. Matter 23, 284116 (2011).

[80] M. Rubinstein and R. H. Colby, Polymer Physics (Oxford University Press, New York, 2003).

[81] M. E. Helgeson, "Colloidal behavior of nanoemulsions: Interactions, structure, and rheology," Curr. Opin. Colloid Interface Sci. 25, 39–50 (2016).

[82] C. R. Seager and T. G. Mason, "Slippery diffusion-limited aggregation," Phys. Rev. E 75, 011406 (2007).

[83] S. Babu, J.-C. Gimel, and T. Nicolai, "Diffusion limited cluster aggregation with irreversible slippery bonds," Eur. Phys. J. E 27, 297–308 (2008).

[84] M. Lin, H. Lindsay, D. Weitz, R. Ball, R. Klein, and P. Meakin, "Universality in colloid aggregation," Nature 339, 360–362 (1989).

[85] C. J. Dimitriou, L. Casanellas, T. J. Ober, and G. H. McKinley, "Rheo-PIV of a shear-banding wormlike micellar solution under large amplitude oscillatory shear," Rheol. Acta 51, 395–411 (2012).

[86] M. A. Calabrese, S. A. Rogers, L. Porcar, and N. J. Wagner, "Understanding steady and dynamic shear banding in a model wormlike micellar solution," J. Rheol. 60, 1001–1017 (2016).

[87] R. Blaak, S. Auer, D. Frenkel, and H. Löwen, "Crystal nucleation of colloidal suspensions under shear," Phys. Rev. Lett. 93, 068303 (2004).

[88] P. Ballesta, N. Koumakis, R. Besseling, W. C. Poon, and G. Petekidis, "Slip of gels in colloid–polymer mixtures under shear," Soft Matter 9, 3237–3245 (2013).

[89] Y. Kobayashi, N. Arai, and A. Nikoubashman, "Structure and dynamics of amphiphilic janus spheres and spherocylinders under shear," Soft Matter 16, 476–486 (2020).

[90] M. M. Talukdar, I. Vinckier, P. Moldenaers, and R. Kinget, "Rheological characterization of xanthan gum and hydroxypropylmethyl cellulose with respect to controlled-release drug delivery," J. Pharm. Sci. 85, 537–540 (1996).

[91] V. Mitsoulas, S. Varchanis, Y. Dimakopoulos, and J. Tsamopoulos, "Dynamics and apparent permeability of the glycocalyx layer: Start-up and pulsating shear experiments in silico," Phys. Rev. Fluids 7, 013102 (2022).

[92] J. P. Sullivan and A. Bose, "On the connection between slurry rheology and electrochemical performance of graphite anodes in lithium-ion batteries," Electrochem. Commun. 141, 107353 (2022).

[93] T. Lombardo, A. C. Ngandjong, A. Belhcen, and A. A. Franco, "Carbon-binder migration: A three-dimensional drying model for lithium-ion battery electrodes," Energy Storage Mater. 43, 337–347 (2021).

28 July 2023 15:49:50